ACS APPLIED MATERIALS & INTERFACES

Research Article

www.acsami.org

Highly Sensitive Detection of Quantal Dopamine Secretion from Pheochromocytoma Cells Using Neural Microelectrode Array Electrodeposited with Polypyrrole Graphene

Li Wang,[†,‡] Huiren Xu,[†,‡] Yilin Song,[†] Jinping Luo,[†] Wenjing Wei,[†,‡] Shengwei Xu,[†] and Xinxia Cai*[,†,‡]

[†]State Key Laboratory of Transducer Technology, Institute of Electronics Chinese Academy of Sciences, Beijing 100190, China

[‡]University of Chinese Academy of Sciences, Beijing 100190, China

ABSTRACT: For the measurement of events of dopamine (DA) release as well as the coordinating neurotransmission in the nerve system, a neural microelectrode array (nMEA) electrodeposited directionally with polypyrrole graphene (PG) nanocomposites was fabricated. The deposited graphene significantly increased the surface area of working electrode, which led to the nMEA (with diameter of 20 μm) with excellent selectivity and sensitivity to DA. Furthermore, PG film modification exhibited low detection limit (4 nM, S/N = 3.21), high sensitivity, and good linearity in the presence of ascorbic acid (e.g., 13933.12 μA mM^{-1} cm^{-2} in the range of 0.8−10 μM). In particular, the nMEA combined with the patch-clamp system was used to detect quantized DA release from pheochromocytoma cells under 100 mM K^+ stimulation. The nMEA that integrates 60 microelectrodes is novel for detecting a large number of samples simultaneously, which has potential for neural communication research.

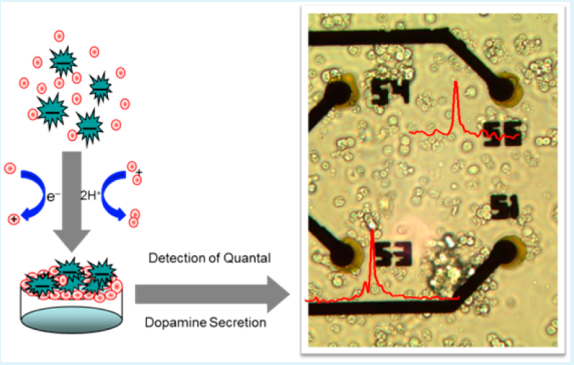

KEYWORDS: *neural microelectrode array, polypyrrole graphene nanocomposites, dopamine, sensitivity, quantal secretion, PC12 cells*

1. INTRODUCTION

Dopamine (DA), a monoamine neurotransmitter released by nerve cells, plays an important role in the human central nervous system. Extracellular concentration of DA in the brain[1,2] is much smaller than that of ascorbic acid (AA) ranging from 200 to 400 μM while their oxidation potentials are extremely close in physiological media (pH 7.4). In addition, dopamine *o*-quinone (the oxidized form of DA) can accelerate the oxidation progress of AA, leading to biosensors with poor selectivity.[3−8] To solve this problem, neurologists have taken a lot of effort to try various modification materials including metal nanoparticles, polymers, enzyme biosensor, carbon nanotubes, graphene (GR),[9−18] and different electrochemical methods such as cyclic voltammetry scanning, chronoamperometry, and differential pulse voltammetry, to achieve high selectivity.[19−22]

Polypyrrole (PPy) is one of the most extensively used conducting polymers in bioanalytical sensors.[23−25] Aside from its biocompatibility, PPy film electrodes exhibit good conductivity doping with cations such as poly(sodium-*p*-styrenesulfonate) (PSS).[26] PPy is also a promising conducting polymer to support the metal nanoparticles.[27−32] A study suggests Au nanoparticles decorated polypyrrole hybrid sheets are ultrasensitive for dopamine detection.[31] However, it also exhibits poor stability and rate capability, which limits its wide application.[29,32]

In recent years, researchers have paid special attention to graphene,[33] which is a novel one-atom thick sp^2-bonded carbon nanomaterial owning unique properties like fast mobility of charge carriers and thermal and chemical stabilities.[34−41] With in-depth research on graphene, many reports are published on the detection of DA in the presence of other similar electroactive chemicals with the electrode modified by graphene. Hasuck Kim's group used glassy carbon electrode (GCE) modified with graphene to detect DA, in the presence of 1 mM AA, and achieved good sensitivity and linearity.[7] GCE modified by a nanocomposite of ß-cyclodextrin and graphene were applied for electrochemical detection of dopamine, which showed low detection limit and broad linear range.[13] A carbon electrode modified by graphene flowers was used to simultaneously determine AA, DA, and uric acid.[42−44] These works are important for improving the technology of detecting DA; however, these sensors do not meet the requirements of miniaturization and quick response for detecting DA exocytosis from single cells.

In this paper, we constructed a high-sensitivity neural microelectrode array (nMEA), fabricated by Micro-Electro-Mechanical-Systems (MEMS) technology and electrodeposited with polypyrrole graphene (PG) nanocomposites. The sensor

Received: January 6, 2015
Accepted: March 25, 2015
Published: March 25, 2015

DOI: 10.1021/acsami.5b00035
ACS Appl. Mater. Interfaces 2015, 7, 7619−7626

Scheme 1. Proposed Mechanism of PG Film Formation

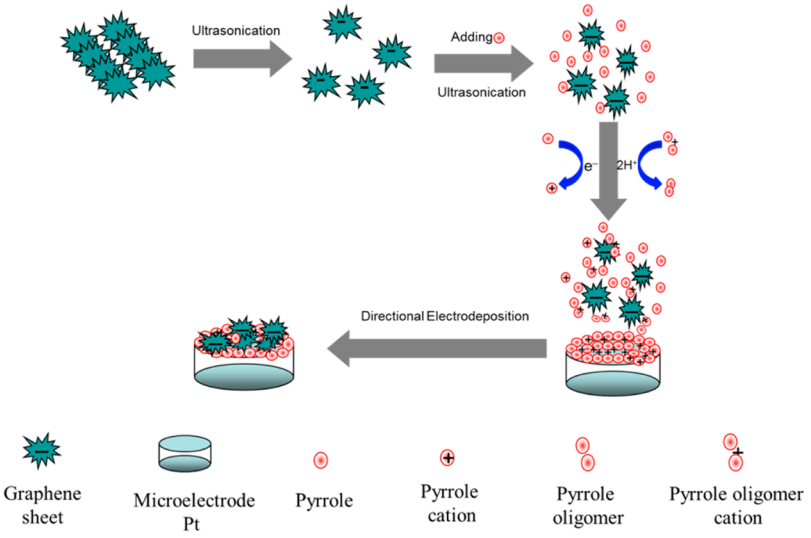

was used for electrochemical detecting of dopamine release from pheochromocytoma cells (PC12) cells, which manifested its great potential for neuroscience research.

2. EXPERIMENTAL SECTION

2.1. Reagents and Instrumentation. Pyrrole (Py) was purchased from Sigma-Aldrich Co., Ltd. Aminated-graphene was obtained from NanoInnova Technologies. NaH_2PO_4 and KCl were purchased from Beijing Chemical Reagents Company (Beijing, China). All reagents were used as received without further purification. Water was purified through a Michem ultrapure water apparatus (Michem, Chengdu, China, resistivity >18 MΩ·cm). PC12 cells were cultured in a CO_2 incubator (SANYO, Japan). Original PC12 cells were purchased from Peking Union Medical College Hospital (Cell Resource Center, CAMS/PUMC, China). Cell buffer solution (that consists of 150 mM NaCl, 2 mM CaCl2, 1.2 mM $MgCl_2$, 5 mM KCl, 11 mM glucose, and 10 mM HEPES, pH 7.2) was freshly prepared prior to use. The phosphate buffer saline (PBS, 0.1 M Na_2HPO_4–NaH_2PO_4–KCl, pH 7.4) was prepared from a PBS tablet (Sigma). Field-emission scanning electron microscopy (FE-SEM) was performed with an Hitachi S-4800 under 5 kV accelerating voltage (Hitachi, Japan). Raman spectra were recorded with a 30 confocal Raman microscope (Tokyo Instruments Co., Japan). All electrochemical measurements were performed on an Autolab PGSTAT302N electrochemical workstation (Autolab, Switzerland). The signals of exocytosis detected by CFE were processed on a patch-clamp system (HEKA, Lambrecht, Germany). The analysis software was Igor Pro 6.1 (WaveMetrics, USA).

2.2. Fabrication of nMEA. The steps involved in the fabrication of nMEA are shown in Figure 2B. The nMEA consists of a glass substrate, a platinum/titanium (Pt/Ti) metal layer, and a silicon nitride (Si_3N_4) layer. A commercialized glass slide (5 cm × 5 cm × 1 mm) was used as the substrate, which was cleaned in turn by acetone, ethanol, and deionized (DI) water. Then a Pt/Ti (200/30 nm) metal mask was patterned onto a substrate followed by ultraviolet photolithograpy.[45,46] The masked glass was placed in an acetone wet etching for several hours. Subsequently, a Si_3N_4 insulating layer (800 nm) was grown onto the substrate using plasma-enhanced chemical vapor deposition. After that, the microelectrode sites were etched in a SF_6-deep reactive ion etcher (SF_6-DRIE) for 10 min at a power of 100 W.[47] The pattern of 60 circular microelectrodes with the diameter of 20 μm and the spacing of 100 μm is used for cell culture and detecting cell secretion. At last, a Plexiglass ring was glued onto the nMEA to form a cell culture dish. The entire fabrication process of the nMEA is in a clean-room environment with MEMs technology.

2.3. Preparation of PG-Modified nMEA. GR (0.5 mg) was sonicated in 1 mL of DI water for 20 min. The aqueous dispersion was mixed with 3.47 μL of Py under ultrasonication for 15 min. The nMEA was polished by O_2-DRIE for 30 s at the power of 50 W, before PG was electrodeposited on the aimed microelectrode of the nMEA by chronopotentiometry. The nMEA was immersed in the above suspension, eight microelectrodes were selected for electrodepositing, and the process was carried out by chronopotentimetry scanning with the charge density of 0.1, 0.2, 0.3, 0.4, 0.5, 0.6, 0.7, and 0.8 C/cm^2 and the current of 2 mA at room temperature. The process is shown in Scheme 1. The obtained microelectrodes were gently washed with DI water to remove excess nonadsorbed species.

2.4. Electrochemical Measurements. The microelectrode performance was measured with an Autolab workstation connected with a computer. A three-electrode system with the selected microelectrode as the working electrode, an Ag|AgCl (saturated KCl) reference electrode, and a platinum wire as the counter electrode was used. Cyclic voltammetry scanning and chronoamperometry were applied to the three-electrode system. Once the background current reached a steady-state value, different doses of DA and AA prepared solutions were injected into the culture dish containing PBS under vigorous stirring. The response currents were recorded with time at a constant applied potential. All experiments were conducted at room temperature.

2.5. Cell Preparation. PC12 cells were companionably provided by Peking Union Medical College Hospital. Cells (1.5 mL) with a density of 10^6 cells/mL were initially planted into a T25 plastic cell culture vessel containing 6 mL of culture medium (5% horse serum and Ham's F12K medium supplemented with 10% fetal bovine serum) at 37 °C in a wet atmosphere of 5% CO_2/95% air. The cells proliferate in culture for 2 days before measuring quantal release test.

2.6. Measurement and Analysis of Quantal Exocytosis. Recordings were used by an HEKA patch-clamp amplifier at room temperature. The matched Patchmaster software was performed at a sampling rate of 10 kHz and the potential of the working site was maintained at 650 mV vs Ag/AgCl. Data analysis of excoytotic spikes was done with software Igor Prov. 6.1 (WaveMetrics, USA) using an algorithm of threshold. A cell secretion occurrence was defined as the maximum current value of a spike being 6 times that of the background noise.

3. RESULTS AND DISCUSSION

3.1. Optimal Electrodeposition Conditions and Mechanism. To properly improve dopamine detection limit and sensitivity with nMEA, PG nanofilm have been used to attempt to modify the microelectrode. The selected 8 among 60

DOI: 10.1021/acsami.5b00035
ACS Appl. Mater. Interfaces 2015, 7, 7619−7626

microelectrodes were electrodeposited with PG film at different charge density from 0.1 to 0.8 C/cm^2, respectively. We identified the optimal electrodeposition conditions through their cyclic voltammetric current response to 20 μM DA solution (solved in PBS, pH 7.2), as shown in Figure 1. In addition to the observed obvious redox peaks, the increment of response current grew with the increase of electrodeposition charge density up to 0.5 C/cm^2. It can be believed that the produced ripples and defects in the layers of the graphene during the electrodepostion process increased the surface area of the electrode and accelerated the electron transfer of the electrode. However, at larger charge density of 0.6 C/cm^2 or more, the current decreased. This result may be attributed to the increase in membrane thickness of PG film as the charge density increased so that the electron generated by the oxidation of substrates from solution could not readily reach the electrode. Thus, we used the charge density of 0.5 C/cm^2 for PG electrodeposition on nMEA.

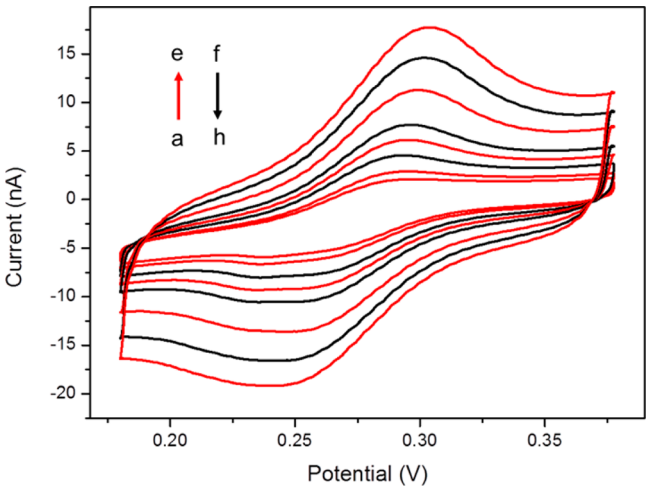

Figure 1. Cyclic voltammetric current response to 20 μM DA at microelectrodes electrodeposited with PG film at different charge densities from 0.1 (a) to 0.8 (h) C/cm^2. The scanning rate was 50 mV/s.

Commonly, when jarless current is applied on a working electrode to provide enough potential, the following electrochemical reactions occur:[46−48]

$$\mathrm{Py} \rightarrow (\mathrm{Py})^+ + \mathrm{e}^-$$

$$2(\mathrm{Py})^+ \rightarrow \mathrm{Py{\cdot}Py} + 2\mathrm{H}^+$$

$$\mathrm{Py{\cdot}Py} \rightarrow (\mathrm{Py{\cdot}Py})^+ + \mathrm{e}^-$$

$$(\mathrm{Py{\cdot}Py})^+ + (\mathrm{Py})^+ \rightarrow \mathrm{Py{\cdot}Py{\cdot}Py} + 3\mathrm{H}^+$$

...

where Py represents a single pyrrole monomer molecule; $(Py)^+$ means radical of pyrrole; Py·Py and Py·Py·Py stands for pyrrole oligomer and $(Py{\cdot}Py)^+$ for pyrrole oligomer cation. Scheme 1 describes the proposed mechanism of PG film. It is believed that the above reaction of pyrrole originally occurs at the Pt microelectrode surface. Like the dispersed graphene containing abundant negative charges, it could be drawn to the pyrrole oligomer cation with positive charge. Afterward, accompanied by a chain of pyrrole polymerization reaction, GR layers would be formed and shaped into folded nanofilm structure, as shown in Figure 2D.

3.2. Characterization of the Electrodeposited PG Nanocomposites on nMEA. To confirm whether it is the PG nanofilm, the Raman spectra measurements[48] have been carried out. Raman spectra were recorded in the range of 800−2000 cm^{-1} using a laser beam having a wavelength of 532 nm with a CCD detector. Figure 2A shows the Raman spectra of PG nanofilm and pure graphene. As for graphene, the specific D band appeared at 1318 cm^{-1} and the G band at 1603 cm^{-1}. However, the D and G bands of PG nanofilm had transferred to 1354 cm^{-1} and the G band at 1610 cm^{-1}. The I_D:I_G (intensity ratio) of graphene was 1.542, while that of PG decreased to 0.887. It means the defects of graphene edge have been repaired while reducing the number of sp^2 hybridization.[49] In addition, bulges at 924, 1007, and 1105 cm^{-1} in the Raman spectra of the PG, related to deformations of N−H and C−H in-plane, has demonstrated the existence of polypyrrole.

As shown in Figure 2D,E, the PG films could be selectively electrodeposited onto the surface of the aimed microelectrodes, and SEM was employed to observe the morphology of the modified working site 1. Large numbers of wrinkles (graphene) and ripples and lots of PPy nanoparticles were grown on the surface of the working site. The observations suggest that the rough and nanostructured PG film provided much larger specific area, which may effectively result in enhancement of electron-transfer capability and consequently increasing the current response.

3.3. Selective Behavior in Electrochemical Detection of AA and DA. *3.3.1. Peak Separation of AA and DA.* Differential pulse voltammetry (DPV) has a better resolution that provides much wider peak separation than cyclic voltammetry. Thus, DPV was used for selective detection of DA and AA on nMEA-electrodeposited PG film. Figure 3 displays DPV of PBS, 5 μM DA, and 5 μM DA in the presence of 800 μM AA using a modified microelectrode. The oxidation current peaks of DA and AA are well-defined separated at the potentials 127 and 273 mV. The calculated oxidation ΔEp is 146 mV for AA and DA, suggesting the modified nMEA exhibits excellent selective performance against DA and AA at the micromolar level. It is believed that electrocatalytic graphene structure[50−52] consisting of amounts of negative charge is effective in attracting the DA cation and rejecting AA anions to the surface of PG nanocomposites.

3.3.2. Responding Speed of PG. The half peak width ($T_{1/2}$) is the duration that the oxidation current spike drops from the maximum to the half-maximum value, which is an important parameter of measuring the response speed. The inset of Figure 3 depicts 3D histograms of these $t_{1/2}$ parameters of DA and AA in the range of 0.6−10 μM. The $t_{1/2}$ of DA was within 0.5 s throughout the entire injection period, while that of AA was more than 1.4 s. Moreover, the response time of AA was 10 times that of DA in the same concentration. Such a distinct response to DA and AA may be attributed as follows: (1) as described before, the large number of negative charges stacked on the PG membrane, which served as a negative surface, making AA anion difficult close; (2) the electron transfer between DA and graphene is more feasible through interaction since DA has phenyl moiety unlike AA.

3.3.3. Current Response of DA and AA in a Mixture with Finite Difference Method. To determine the selectivity and sensitivity of the microelectrode electrodeposited with PG film, the current response of DA was recorded in the presence of a high concentration of AA (the concentration of AA was maintained at 100 times that of DA). As shown in Figure 4A,

DOI: 10.1021/acsami.5b00035
ACS Appl. Mater. Interfaces 2015, 7, 7619−7626

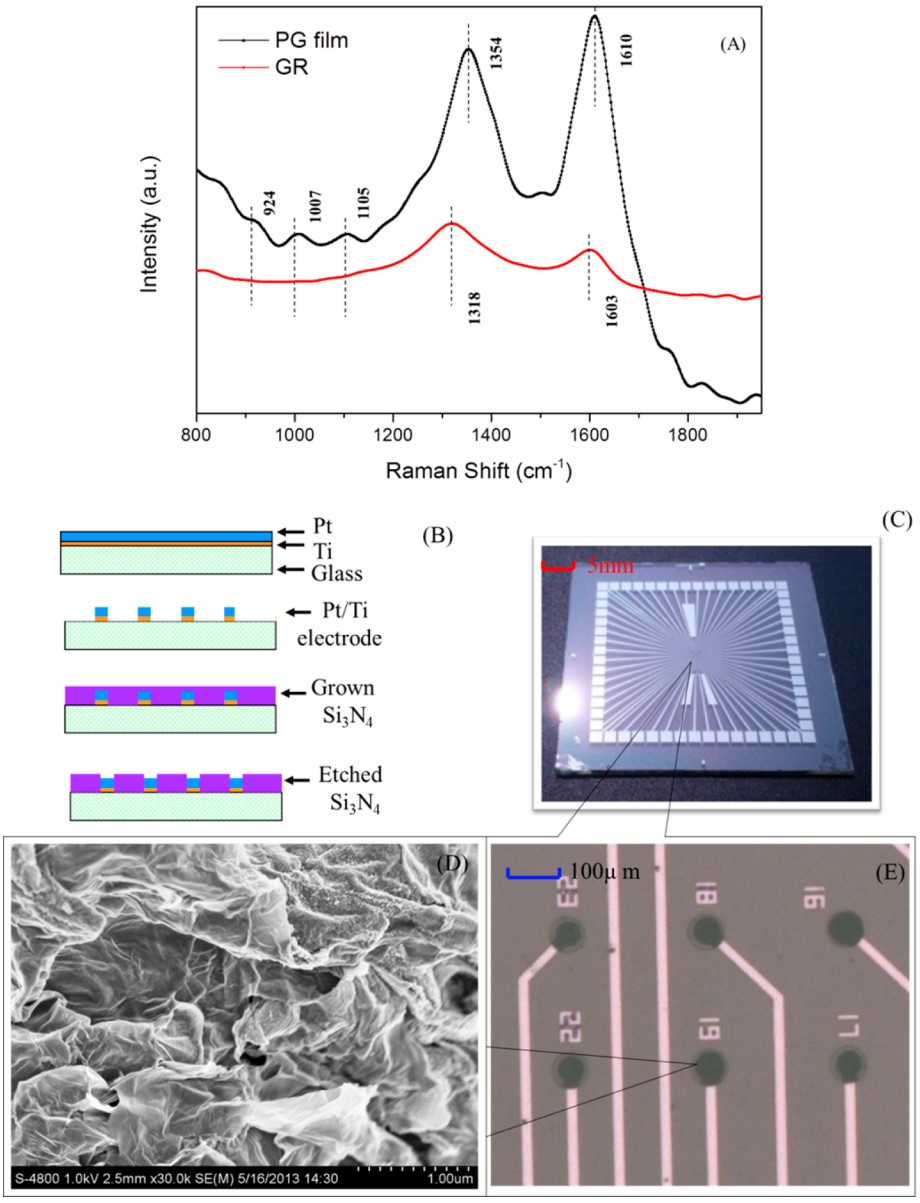

Figure 2. (A) Raman spectra of PG nanocomposites and pure graphene (GR); (B) fabrication process of the nMEA; (C) nMEA with 60 working sites in the center of the glass slide substrate; (D) SEM image of the modified microelectrode; (E) microelectrodes selectively electrodeposited with PG films on the nMEA.

we selected one microelectrode nMEA electrodeposited with PG film as the working microelectrode for amperometric detection in two steps. The potential was held at 273 mV vs Agl AgCl which was the oxidation peak potential of DA. The first step was stepwise addition of different concentrations of DA in the presence of high concentration AA to a stirred solution; the concentrations were prepared as follows: 0.8 μM + 80 μM (DA + AA), 1.0 μM + 0.1 mM, 2.0 μM + 0.2 mM, 4.0 μM + 0.4 mM, 6.0 μM + 0.6 mM, 8.0 μM + 0.8 mM, and 10 μM + 1 mM. The second step consisted of different concentrations of AA being injected into the PBS solution in sequence of 80 μM, 0.1 mM, 0.2 mM, 0.4 mM, 0.6 mM, 0.8 mM, and 1.0 mM. The response current of DA in the presence of AA minus the response current of AA in the same concentration was equal to the current of DA. Figure 4B displayed the current response of DA, by subtracting the response current of AA from the response current of DA in the presence of AA, increasing linearly with their concentrations having a correlation coefficient of 0.991. Similarly, the sensitivity of DA was 0.161 nA/μM (12818.47 μA mM^{-1} cm^{-2}). To properly reflect the performance of the microelectrode array modified with PG film, 8 microelectrodes among 60 microelectrodes were selected to detect DA in the presence of AA. The coefficient of variation is less than 2.7%.The results showed the sensitivity of the nMEA modified by PG film for DA and AA differed dramatically, which may be attributed to the following: (1) the rough PG film with lots of wrinkles enlarging the surface size (the effective surface area of electrode modified with PG film is 1264.69 μm^2 calculated by Randles-Sevcik equation using $K_3Fe(CN)_6/K_4Fe(CN)_6$ as an indicator) greatly increases their electrocatalytic active sites and accelerates a chemical reaction; (2) PG film with a large number of sp^2 bonds can provide more free electrons and promote the electron transfer in the oxidation of DA.

3.4. Detection Limit of Dopamine. To further characterize the performance of the nMEA modified with PG nanocomposites, we determined the detection limit of DA

DOI: 10.1021/acsami.5b00035
ACS Appl. Mater. Interfaces 2015, 7, 7619−7626

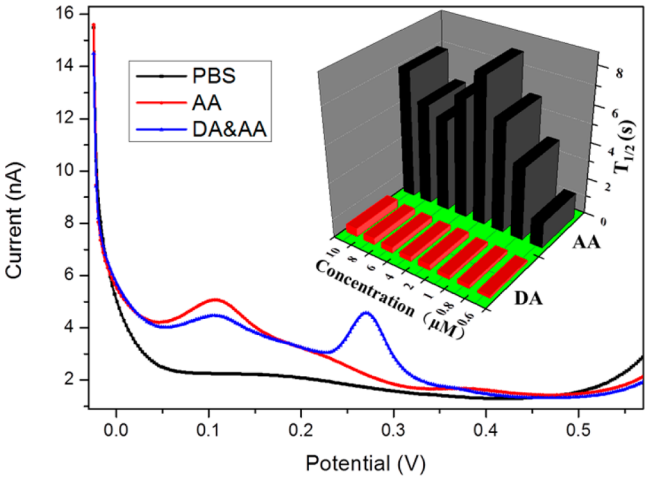

Figure 3. DPV of PBS, 800 μM AA, and 5 μM DA in the presence of 800 μM AA on nMEA-electrodeposited PG film. The inset shows 3D-histograms of the $t_{1/2}$ parameter of DA and AA in the range of 0.6−10 μM.

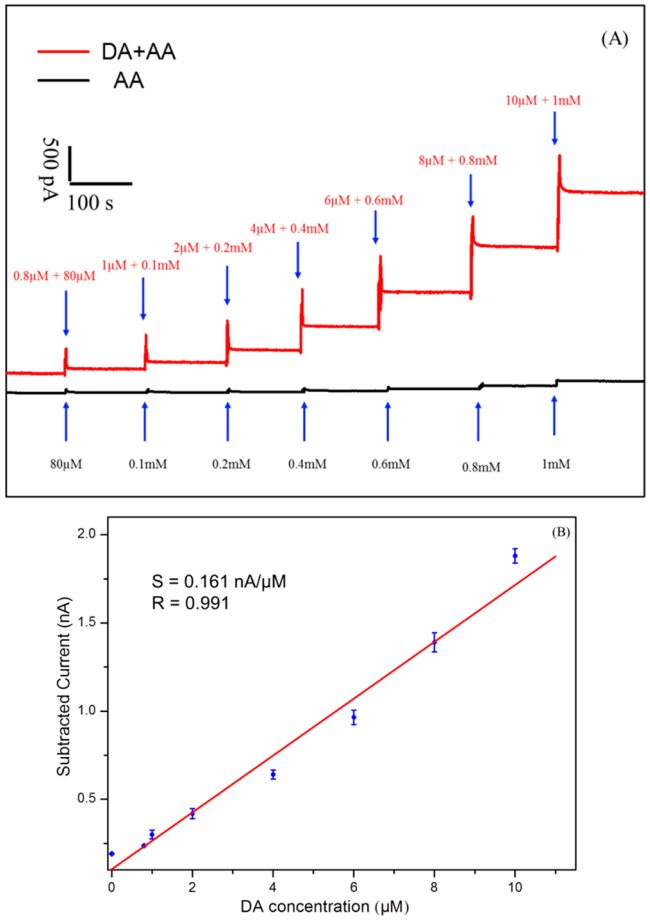

Figure 4. (A) Amperometric responses of AA and DA in the presence of 100-fold concentration of AA on the microelectrode modified with PG film at the working potential of 273 mV vs AglAgCl. (B) The linership between the differential currents and the DA concentration.

(LOD). A stepwise current−time response of the nMEA at different DA concentrations was obtained as shown in Figure 5. Twenty microliters of PBS was added first to the PBS solution to eliminate the influence of diffusion-limited responses from PBS. An obvious gradient current response of DA at the

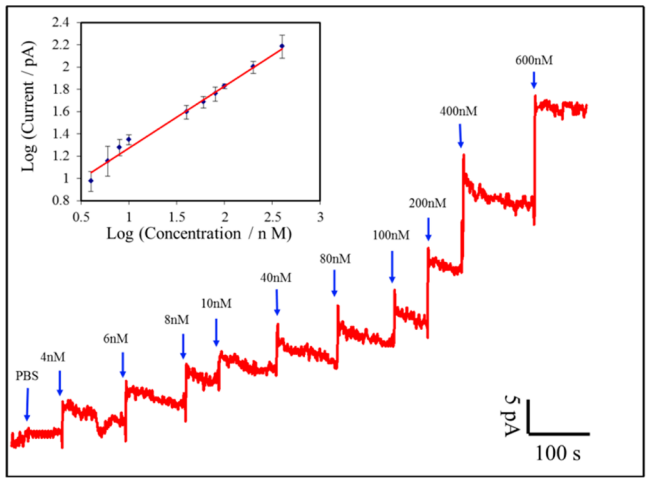

Figure 5. Amperometric responses of dopamine in the range of 4−600 nM on the nMEA electrodeposited with PG film. Applied potential: 273 mV vs AglAgcl. The inset shows the logarithm plot of current versus concentration of DA.

nanomolar level ranging from 4 to 600 nM and the oxidation current of 4 nM is about 6.3 pA with adequate resolution (S/N = 3.21), which is better than that of previously reported work using GR.[13] The relationship between current responses and concentration of DA can be represented by a sigmoidal equation.

$$I = 5.216C^{0.556}$$

where I stands for an anodic current and C is the DA concentration. Such fixed equation for I vs C is inconvenient to use, so we used the logarithm of the coordinate axes of the calibration curve to generate a linear relationship. The slope of the linear curve represents the sensitivity of the electrode. The defined sensitivity of nMEA-electrodeposited PG film was 0.557 log (pA)/log (nM) with a correlation coefficient of 0.986, as shown in the inset in Figure 5. The figures of merit toward DA detection obtained with some other reported graphene materials are summarized in Table 1. As compared in Table 1, the present microelectrode modified with PG film demonstrated better properties of electrochemical detection of DA than those of other graphene samples.

3.5. Monitoring of Dopamine Release from PC12 Cells. PC12 cell can synthesize neurotransimitters (mainly DA), stock catecholamine-containing vesicles, release, and pass

Table 1. Comparison of Analytical Performance of Our Modified nMEA with Other Published DA Electrode Based on Graphene-Based Materials

materials	limit of detection	linear range	references
reduced graphene oxide	2 μM	5−200 μM	4
graphene	2.64 μM	4−100 μM	7
carbon paste electrode	3.70 μM	8−134 μM	8
reduced graphene-P pPD	0.36 μM	5−25 μM	35
N-doped reduced graphene oxide	0.25 μM	5−170 μM	41
graphene nanosheet	0.6 μM	4−52 μM	52
reduced graphene oxide	0.5 μM	0.5−60 μM	40
3D-reduced graphene oxide	0.17 μM	0.5−1 mM	53
polypyrrole graphene	4 nM	0.8−10 μM	this study

DOI: 10.1021/acsami.5b00035
ACS Appl. Mater. Interfaces 2015, 7, 7619−7626

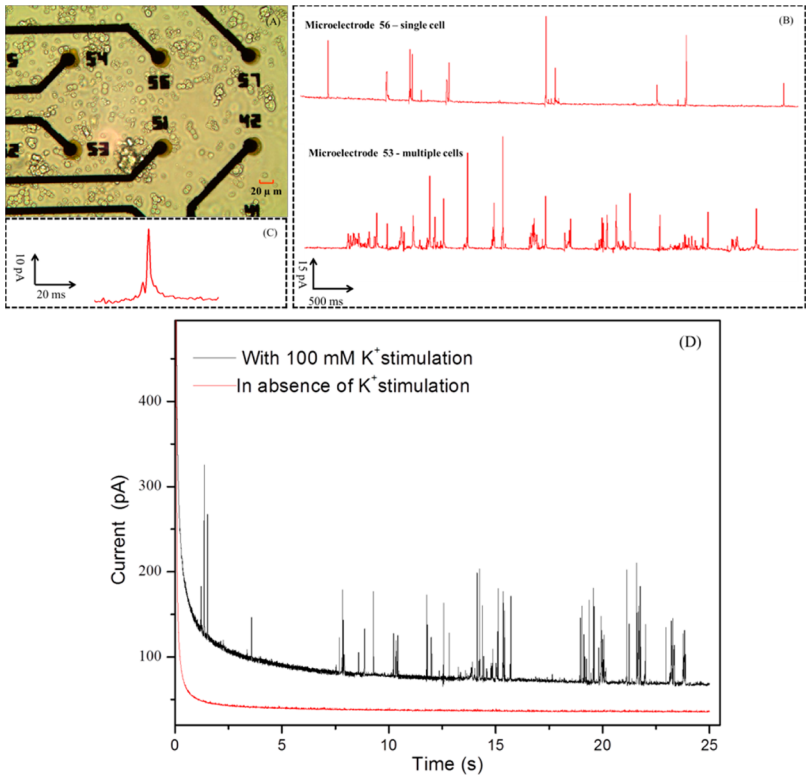

Figure 6. (A) Sample photomicrograph that shows microelectrodes are occupied by PC12 cells. (B) Amperometric traces of single cell and multiple cells are recorded on microelectrode 56 and microelectrode 53, respectively, at the potential of 273 mV vs AglAgCl, with 100 mM K^+ stimulation solution. (C) A typical spike separate from microelectrode 56. (D) The two traces are recorded by amperometric method with K^+ stimulation and in the absence of K^+ stimulation, respectively.

to receptors of postsynaptic membrane, so it has been generally used as a model for researching DA release in vitro.[54−58]

As can be seen in Figure 6A, the optical inverted photomicrograph indicates that among 6 microelectrodes used in the experiment, 5 electrodes are occupied by PC12 cells following cell washing with cell buffer solution (that consists of 150 mM NaCl, 2 mM $CaCl_2$, 1.2 mM $MgCl_2$, 5 mM KCl, 11 mM glucose, and 10 mM HEPES, pH 7.2). The nMEA that the PC12 cells cultured was placed into the self-made interface, which combines with HKEA amplifier. We chose the microelectrodes occupied by single cell and multiple cells as the targets for monitoring dopamine release, such as microelectrodes 56 and 53 in Figure 6A. Typical amperometric traces of single cell and multiple cells are presented in Figure 6B. Many upward current spikes are detected after the introduction of high K^+ stimulus to trigger exocytosis. The reason for it is that an increased extracellular high concentration of K^+ provokes the depolarization of dopaminergic neurons and so triggers exocytosis by opening specific-binding Na^+ entry, which induces the subsequent opening of voltage-sensitive Ca^{2+} channels. The opening of Ca^{2+} channels allows a quick influx of Ca^{2+} concentration in the intracellular level to a level sufficient to provoke the transferring of neurotransmitter-containing vesicles to the plasma membrane for exocytosis.[58−61]

A typical spike was observed as shown in Figure 6C. The exocytosis occurs in a stepwise fashion. The initial event observed is the foot signal recorded from the initial leakage of dopamine from the membrane-fused vesicle, which may then progress into the sharp fusion pore and release of the major dopamine content.[46,62−66]

To ascertain whether DA release caused by high concentrations of K^+ stimulation solution, two group tests were performed at a sampling rate of 10 kHz as shown in Figure 6D. No DA release events described as a succession of amperometric spikes were recorded from the PC12 cells in the absence of an appropriate stimulus; however, dense spikes responses were observed, proving that the cell was triggered to release dopamine by adding a 100 mM K^+ stimulation solution.

3.6. Stablility of nMEA Modified with PG Films. The stability of the nMEA electrodeposted PG film was studied by keeping the nMEA in PBS at 4 °C for 50 days after having been used for detecting DA release from single PC12 cells. Over the first 7 days, the sensitivity of DA decreased by 2.3% and the detection limit was 10 nM. The sensitivity of DA maintained 91.1% of the original sensitivity value after 50 days. These results indicate that the nMEA-electrodeposited PG film displayed stable and excellent response to dopamine.

4. CONCLUSIONS

In this work, a novel nMEA electrodeposited with PG nanocomposites was fabricated and used for highly sensitive detection of DA exocytosis in vitro. The novel nMEA showed outstanding selectivity between DA and AA. Large peak potential separation and high peak current between DA and AA could be obtained using DPV at the modified nMEA. Meanwhile, the electrodeposited nMEA exhibited superior sensitivity, low detection limit, and fast responding speed toward the oxidation of DA. The splendid performance was due to fast approaching microelectrode steady state and the promoted electron-transfer ability of GR. Additionally, we applied the nMEA modified with the PG nanocomposites for

DOI: 10.1021/acsami.5b00035
ACS Appl. Mater. Interfaces 2015, 7, 7619−7626

detecting DA release from PC12 cells, which has great potential in electrochemical neuroscience.

AUTHOR INFORMATION

Corresponding Author

*E-mail: xxcai@mail.ie.ac.cn. Tel.: +86-10-58887193. Fax: +86-10-58887172.

Notes

The authors declare no competing financial interest.

ACKNOWLEDGMENTS

This work was sponsored by the NSFC (No. 61125105, No. 61101048); the Major National Scientific Research Plan (2011CB933202, 2014CB74465); the Beijing Municipal Science & Technology Commission (Z141102003414014).

REFERENCES

(1) LaVoie, M.; Ostaszewski, B.; Weihofen, A.; Schlossmacher, M.; Selkoe, J. Dopamine covalently modifies and functionally inactivates parkin. *Nat. Med.* **2005**, *11*, 1214−1221.

(2) Borland, L. M.; Michael, A. C. *Electrochemical methods for neuroscience*; Taylor and Francis: London, 2006; Chapter 1, pp 1−15.

(3) Wightman, R. M.; May, L. J.; Michael, A. Detection of dopamine dynamics in the brain. *J. Am. Chem. Soc.* **1988**, *60*, 769A−793A.

(4) Wang, Y.; Li, Y.; Tang, L.; Lu, J.; Li, J. Application of graphene-modified electrode for selective detection of dopamine. *Electrochem. Commun.* **2009**, *11*, 889−892.

(5) Wei, D.; Bailey, M. J. A.; Andrew, P.; Ryhänen, T. Electrochemical biosensors at the nanoscale. *Lab Chip* **2009**, *9*, 2123−2131.

(6) Mendez, I.; Vinuela, A.; Astradsson, A.; Mukhida, K.; Hallett, P.; Robertson, H.; Tierney, T.; Holness, R.; Dagher, A.; Trojanowski, J. Q.; Isacson, O. Dopamine neurons implanted into people with Parkinson's disease survive without pathology for 14 years. *Nat. Med.* **2008**, *14*, 507−509.

(7) Kim, Y. R.; Bong, S.; Kang, Y.-J.; Yang, Y.; Mahajan, R. K.; Kim, J. S.; Kim, H. Electrochemical detection of dopamine in the presence of ascorbic acid using graphene modified electrodes. *Biosens. Bioelectron.* **2010**, *25*, 2366−2369.

(8) Colin-Orozco, E.; Ramirez-Silva, M. T.; Corona-Avendano, S.; Romero-Romo, M.; Palomar-Pardave, M. Electrochemical quantification of dopamine in the presence of ascorbic acid and uric acid using a simple carbon paste electrode modified with SDS micelles at pH 7. *Electrochim. Acta* **2012**, *85*, 307−313.

(9) Schmidt, A. C.; Wang, X.; Zhu, Y.; Sombers, L. A. Carbon Nanotube Yarn Electrodes for Enhanced Detection of Neurotransmitter Dynamics in Live Brain Tissue. *ACS Nano* **2013**, *7*, 7864−7873.

(10) Geim, A. K. Graphene: Status and Prospects. *Science* **2009**, *19*, 1530−1534.

(11) Chao, C.; Liu, J.; Wang, J.; Zhang, Y.; Zhang, B.; Zhang, Y.; Xiang, X.; Chen, R. Surface modification of halloysite nanotubes with dopamine for enzyme immobilization. *ACS Appl. Mater. Interfaces* **2013**, *5*, 10559−10564.

(12) Reckinger, N.; Van Hooijdonk, E.; Joucken, F.; Tyurnina, A. V.; Lucas, S.; Colomer, J.-F. Anomalous moiré pattern of graphene investigated by scanning tunneling microscopy: Evidence of graphene growth on oxidized Cu. *Nano Res.* **2014**, *7*, 154−162.

(13) Du, J.; Yue, R.; Ren, F.; Yao, Z.; Jiang, F.; Yang, P.; Du, Y. Novel graphene flowers modified carbon fibers for simultaneous determination of ascorbic acid, dopamine and uric acid. *Biosens. Bioelectron.* **2014**, *53*, 220−224.

(14) Liang, W.; He, S.; Fang, J. Self-Assembly of J-Aggregate Nanotubes and Their Applications for Sensing Dopamine. *Langmuir* **2014**, *30*, 805−811.

(15) Kelly, K. L.; Coronado, E.; Zhao, L. L. The optical properties of metal nanoparticles: the influence of size, shape, and dielectric environment. *J. Phys. Chem. B* **2003**, *10*, 668−677.

(16) Sansuk, S.; Bitziou, E.; Covington, J. A.; Joseph, M. B.; Boutelle, M. G.; Unwin, P. R.; Macpherson, J. V. Ultrasensitive detection of dopamine using a carbon nanotube network microfluidic flow electrode. *Anal. Chem.* **2012**, *85*, 163−169.

(17) Yang, Z.-H.; Zhuo, Y.; Chai, Y.-Q.; Yuan, R. High throughput immunosensor based on multi-label strategy and a novel array electrode. *Sci. Rep.* **2014**, *4*, 1−7.

(18) Liu, M.; Liu, X.; Wang, J.; Wei, Z.; Jiang, L. Electromagnetic synergetic actuators based on polypyrrole/Fe_3O_4 hybrid nanotube arrays. *Nano Res.* **2010**, *3*, 670−675.

(19) Howe, M. W.; Tierney, P. L.; Sandberg, S. G.; Phillips, P. E. M.; Graybiel, A. M. Prolonged dopamine signalling in striatum signals proximity and value of distant rewards. *Nature* **2013**, *500*, 575−579.

(20) Jennings, K. A. A Comparison of the subsecond dynamics of neurotransmission of dopamine and serotonin. *ACS Chem. Neurosci.* **2013**, *4*, 704−714.

(21) Stuber, G. D.; Klanker, M.; de Ridder, B.; Bowers, M. S.; Joosten, R. N.; Feenstra, M. G.; Bonci, A. Reward-predictive cues enhance excitatory synaptic strength onto midbrain dopamine neurons. *Science* **2008**, *321*, 1690−1692.

(22) Taylor, I. M.; Ilitchev, A. I.; Michael, A. C. Restricted diffusion of dopamine in the rat dorsal striatum. *ACS Chem. Neurosci.* **2013**, *4*, 870−878.

(23) Wang, J.; Botelho, S. J.; Naguib, H. E.; Bazylak, A. Development of a Novel Active Polypyrrole Trilayer Membrane. *ACS Sustainable Chem. Eng.* **2013**, *1*, 226−231.

(24) Jager, E.; Smela, E.; Inganäs, O. Microfabricating conjugated polymer actuators. *Science* **2000**, *290*, 1540−1545.

(25) Milczarek, G.; Inganas, O. Renewable cathode materials from biopolymer/conjugated polymer interpenetrating networks. *Science* **2012**, *23*, 1468−1471.

(26) Khomenko, V. G.; Barsukov, V. Z.; Katashinskii, A. S. The catalytic activity of conducting polymers toward oxygen reduction. *Electrochim. Acta* **2005**, *50*, 1675−1683.

(27) Ulubay, Ş.; Dursun, Z. Cu nanoparticles incorporated polypyrrole modified GCE for sensitive simultaneous determination of dopamine and uric acid. *Talanta* **2010**, *80*, 1461−1466.

(28) Feng, X.; Zhang, Y.; Zhou, J.; Li, Y.; Chen, S.-F.; Zhang, L.; Ma, Y.; Wang, L.-H.; Yan, X. Three-dimensional nitrogen-doped graphene as an ultrasensitive electrochemical sensor for the detection of dopamine. *Nanoscale* **2015**, *7*, 2427−2432.

(29) Burgoyne, H. A.; Kim, P.; Kolle, M.; Epstein, A. K.; Aizenberg, J. Screening conditions for rationally engineered electrodeposition of nanostructures (SCREEN): electrodeposition and applications of polypyrrole nanofibers using microfluidicgradients. *Small* **2012**, *22*, 3502−3509.

(30) Ulubay, S.; Dursun, Z. Cu nanoparticles incorporated polypyrrole modified GCE for sensitive simultaneous determination of dopamine and uric acid. *Talanta* **2010**, *80*, 1461−1466.

(31) Qian, T.; Yu, C.; Zhou, X.; Wu, S.; Shen, J. Au nanoparticles decorated polypyrrole/reduced graphene oxide hybrid sheets for ultrasensitive dopamine detection. *Sens. Actuators, B* **2014**, *193*, 759−763.

(32) Zhang, D.; Zhang, X.; Chen, Y.; Yu, P.; Wang, C.; Ma, Y. Enhanced capacitance and rate capability of graphene/polypyrrole composite as electrode material for supercapacitors. *J. Power Sources* **2011**, *196*, 5990−5996.

(33) Withers, F.; Bointon, T. H.; Craciun, M. F.; Russo, S. All-graphene photodetectors. *ACS Nano* **2013**, *7*, 5052−5057.

(34) Liu, S.; Yu, B.; Zhang, T. Preparation of crumpled reduced graphene oxide-poly (p-phenylenediamine) hybrid for the detection of dopamine. *J. Mater. Chem.* **2013**, *A1*, 13314−13320.

(35) Novoselov, K. S.; Geim, A. K.; Morozov, S. V.; Jiang, D.; Katsnelson, M. I.; Grigorieva, I. V.; Dubonos, S. V.; Firsov, A. A. Two-dimensional gas of massless Dirac fermions in graphene. *Nature* **2005**, *438*, 197−200.

(36) Liu, D.; Zhang, X.; You, T. Electrochemical Performance of Electrospun Free-Standing Nitrogen-Doped Carbon Nanofibers and

DOI: 10.1021/acsami.5b00035
ACS Appl. Mater. Interfaces 2015, 7, 7619−7626

Their Application for Glucose Biosensing. *ACS Appl. Mater. Interfaces* **2014**, *6*, 6275−6280.
(37) Tang, L.; Wang, Y.; Li, Y.; Feng, H.; Lu, J.; Li, J. Preparation, structure, and electrochemical properties of reduced graphene sheet films. *Adv. Funct. Mater.* **2009**, *19*, 2782−2789.
(38) Lee, J.; Tan, J. Y.; Toh, C.-T.; Koenig, S. P.; Fedorov, V. E.; Castro Neto, A. H.; Barbaros, O. Nanometer thick elastic graphene engine. *Nano Lett.* **2014**, 2677−2680.
(39) Robinson, J.; Trumbull, K.; Cavalero, R.; Weng, X.; Wetherington, M.; Frantz, E.; Labella, M.; Hughes, Z.; Fanton, M.; Snyder, D. Nucleation of epitaxial graphene on SiC (0001). *ACS Nano* **2009**, *4*, 153−158.
(40) Sheng, Z.-H.; Zheng, X.-Q.; Xu, J.-Y.; Bao, W.-J.; Wang, F.-B.; Xia, X.-H. Electrochemical sensor based on nitrogen doped graphene: simultaneous determination of ascorbic acid, dopamine and uric acid. *Biosens. Bioelectron.* **2012**, *34*, 125−131.
(41) Tan, L.; Zhou, K. G.; Zhang, Y. H.; Wang, H. X.; Wang, X. D.; Guo, Y. F.; Zhang, H. L. Nanomolar detection of dopamine in the presence of ascorbic acid at *β*-cyclodextrin/graphene nanocomposite platform. *Electrochem. Commun.* **2010**, *124*, 557−560.
(42) Liu, S.-Q.; Sun, W.-H.; Hu, F.-T. Graphene nano sheet-fabricated electrochemical sensor for the determination of dopamine in the presence of ascorbic acid using cetyltrimethylammonium bromide as the discriminating agent. *Sens. Actuators, B* **2012**, *173*, 497−504.
(43) Yang, L.; Liu, D.; Huang, J.; You, T. Simultaneous determination of dopamine, ascorbic acid and uric acid at electrochemically reduced graphene oxide modified electrode. *Sens. Actuators, B* **2014**, *193*, 166−172.
(44) Barizuddin, S.; Liu, X.; Mathai, J. C.; Hossain, M.; Gillis, K. D.; Gangopadhyay, S. Automated targeting of cells to electrochemical electrodes using a surface chemistry approach for the measurement of quantal exocytosis. *ACS Chem. Neurosci.* **2010**, *1*, 590−597.
(45) Spegel, C.; Heiskanen, A.; Pedersen, S.; Emneus, J.; Ruzgas, T.; Taboryski, R. Fully automated microchip system for the detection of quantal exocytosis from single and small ensembles of cells. *Lab Chip* **2008**, 323−329.
(46) Li, Y. Effect of anion concentration on the kinetics of electrochemical polymerization of pyrrole. *J. Electroanal. Chem.* **1997**, *433*, 181−186.
(47) Garfias-García, E.; Romero-Romo, M.; Ramírez-Silva, M.T.; Palomar-Pardavé, M. Mechanism and kinetics of the electrochemical formation of polypyrrole under forced convection conditions. *J. Electroanal. Chem.* **2008**, *613*, 67−79.
(48) Álvarez-Romero, G. A.; Garfias-García, E.; Ramírez-Silva, M. T.; Galán-Vidal, C.; Romero-Romo, M.; Palomar-Pardavé, M. Electrochemical and AFM characterization of the electropolimerization of pyrrole over a graphite−epoxy resin solid composite electrode, in the presence of different anions. *Appl. Surf. Sci.* **2006**, *252*, 5783−5792.
(49) Raman, A. Ternary FeB- and CrB-type phases with yttrium, lanthanum, and some rare earths. *Inorg. Chem.* **1968**, *75*, 973−976.
(50) Bose, S.; Kuila, T.; Uddin, M. E.; Kim, N. H.; Lau, A. K. T.; Lee, J. H. In-situ synthesis and characterization of electrically conductive polypyrrole/graphene nanocomposites. *Polymer* **2010**, *51*, 5921−5928.
(51) Liu, X.; Barizuddin, S.; Shin, W.; Mathai, C. J.; Gangopadhyay, S.; Gillis, K. D. Microwell device for targeting single cells to electrochemical microelectrodes for high-throughput amperometric detection of quantal exocytosis. *Anal. Chem.* **2011**, *83*, 2445−2451.
(52) Keeley, G. P.; O'Neill, A.; McEvoy, N.; Peltekis, N.; Coleman, J. N.; Duesberg, G. S. Electrochemical ascorbic acid sensor based on DMF-exfoliated graphene. *J. Mater. Chem.* **2010**, *20*, 7864−7869.
(53) Yang, L.; Liu, D.; Huang, J.; You, T. Simultaneous determination of dopamine, ascorbic acid and uric acid at electrochemically reduced graphene oxide modified electrode. *Sens. Actuators, B* **2014**, *193*, 166−172.
(54) Yu, B.; Kuang, D.; Liu, S.; Liu, C.; Zhang, T. Template-assisted self-assembly method to prepare three-dimensional reduced graphene oxide for dopamine sensing. *Sens. Actuators, B* **2014**, *205*, 120−126.
(55) Chang, L.; Howdyshell, M.; Liao, W.-C.; Chiang, C.-L.; Gallego-Perez, D.; Yang, Z.; Lu, W.; Byrd, J. C.; Muthusamy, N.; Lee, L. J.; Sooryakumar, R. Magnetic Tweezers-Based 3D Microchannel Electroporation for High-Throughput Gene Transfection in Living Cells. *Small* **2014**, *1*, 1−11.
(56) Auerbach, A. A. Spontaneous and evoked quantal transmitter release at a vertebrate central synapse. *Nature* **1971**, *234*, 181−183.
(57) Feng, X.; Zhang, Y.; Yan, Z.; Chen, N.; Ma, Y.; Liu, X.; Yang, X.; Hou, W. Self-degradable template synthesis of polyaniline nanotubes and their high performance in the detection of dopamine. *J. Mater. Chem. A* **2013**, *1*, 9775−9780.
(58) Wightman, R. M.; Jankowski, J. A.; Kennedy, R. T.; Kawagoe, K. T.; Schroeder, T. J.; Leszczyszyn, D. J.; Near, J. A.; Diliberto, E. J.; Viveros, O. H. Temporally resolved catecholamine spikes correspond to single vesicle release from individual chromaffin cells. *Proc. Natl. Acad. Sci. U. S. A.* **1991**, *88*, 10754−10758.
(59) Wang, L.; Xu, H; Song, Y; Luo, J.; Xu, S; Zhang, S; Liu, J.; Cai, X. Carbon Fiber Ultramicrodic Electrode Electrodeposited with Over-Oxidized Polypyrrole for Amperometric Detection of Vesicular Exocytosis from Pheochromocytoma Cell. *Sensors* **2015**, *15*, 868−879.
(60) Meunier, A.; Fulcrand, R.; Darchen, F. M.; Collignon, M. G.; Lemaître, F.; Amatore, C. Indium tin oxide devices for amperometric detection of vesicular release by single cells. *Biophys. Chem.* **2012**, *16*, 214−221.
(61) Bae, J.; Song, M. K.; Park, Y. J.; Kim, J. M.; Liu, M.; Wang, Z. L. Fibre supercapacitors made of nanowire−fibre hybrid structures for wearable/flexible energy storage. *Angew. Chem., Int. Ed.* **2011**, *50*, 1683−1687.
(62) Normann, R. A. Technology insight: future neuroprosthetic therapies for disorders of the nervous system. *Nat. Clin. Pract. Neurol.* **2007**, *3*, 444−452.
(63) Lebedev, M. A.; Tate, A. J.; Hanson, T. L.; Zheng, L.; O'Doherty, J. E.; Winans, J. A.; Ifft, P. J.; Zhuang, K. Z.; Fitzsimmons, N. A.; Schwarz, D. A.; Fuller, A. M.; An, J. H.; Nicolelis, M. A. L. Future developments in brain-machine interface research. *Clinics* **2011**, *66*, 25−32.
(64) Normann, R. A.; Warren, D. J.; Ammermuller, J.; Fernandez, E.; Guillory, S. High-resolution spatio-temporal mapping of visual pathways using multi-electrode arrays. *Vision Res.* **2001**, *41*, 1261−1275.
(65) Huang, Y.; Cai, D.; Chen, P. Micro- and nanotechnologies for study of cell secretion. *Anal. Chem.* **2011**, *83*, 4393−4406.
(66) Spegel, C.; Heiskanen, A.; Acklid, J.; Wolff, A.; Taboryski, R.; Emneus, J. On-Chip Determination of Dopamine Exocytosis Using Mercaptopropionic Acid Modified Microelectrodes. *Electroanalysis* **2007**, *19*, 263−271.

DOI: 10.1021/acsami.5b00035
ACS Appl. Mater. Interfaces 2015, 7, 7619−7626